ASTRONOMY & ASTROPHYSICS
SUPPLEMENT SERIES

Astron. Astrophys. Suppl. Ser. **145**, 305–310 (2000)

Using single-mode fibers to monitor fast Strehl ratio fluctuations

Application to a 3.6 m telescope corrected by adaptive optics

V. Coudé du Foresto[1], **M. Faucherre**[2], **N. Hubin**[3], **and P. Gitton**[3]

[1] Observatoire de Paris/DESPA, 5 place Jules Janssen, 92195 Meudon Cedex, France
[2] 2 rue de la chicane, 34130 Saint-Aunès, France
[3] European Southern Observatory, Karl-Schwarzschildstraβe # 2, D-85748 Garching bei München, Germany

Received September 30, 1999; accepted March 31, 2000

Abstract. The theory of starlight coupling into single-mode fibers is reviewed to show how i) the central obstruction in a telescope pupil deteriorates coupling efficiency much more than one would expect from the loss of collecting area, and ii) a single-mode fiber and a photometer can be used to monitor fast Strehl ratio fluctuations. This last point is illustrated with experimental data obtained at the 3.6 m La Silla telescope corrected with the ADONIS adaptive optics system. A 37× gain in coupling efficiency was demonstrated by turning on the adaptive optics system, but periodic fluctuations in the coupled signal revealed a vibration of the telescope tube that could not have been detected otherwise.

Key words: telescopes — techniques: interferometric, adaptive optics — instrumentation: large telescopes — optical fibers: single-mode — infrared: general

1. Introduction

Single-mode fibers are useful, in the focal plane of seeing limited telescopes, for their spatial filtering capability. The waveguides transform wavefront phase corrugations into intensity fluctuations, thus providing a stable, well-defined output stellar beam with a minimum étendue (λ^2). This property can be used in high resolution spectroscopy (Ge et al. 1998), or to combine high angular and spectral resolution behind adaptive optics, and finally in stellar interferometry (Foresto et al. 1997). The spatial filtering capability, however, comes at a price: from the incoherent wavefront, only part of the light can be coupled into the single-mode waveguide. Thus a key issue with single-mode fibers is the efficiency of their coupling to starlight. Point source to fiber coupling theory is reviewed and illustrated in Sect. 2, for two cases: The wavefront is diffraction (Sect. 2.1) and seeing (Sect. 2.2) limited. It is shown how the coupling coefficient is linked to the instantaneous Strehl ratio. Thus, a single-mode fiber associated to a photometer can be used as a "fast Strehlmeter" to monitor the rapid image quality fluctuations of a dynamic optical system. This is illustrated by experimental data obtained in the K band ($2.0\,\mu\mathrm{m} \leq \lambda \leq 2.4\,\mu\mathrm{m}$) with a 3.6 m telescope corrected by the ADONIS adaptive optics system (Sect. 3).

Send offprint requests to: V. Coudé du Foresto;
e-mail: vincent.foresto@obspm.fr

2. Injecting a point source

Injecting starlight into a fiber is usually achieved in the focal plane of the telescope, by forming an image of the star onto the fiber head. To compute the efficiency we first follow the classical method of the overlap integral, whose details can be found in e.g. (Neumann 1988) or (Jeunhomme 1993).

A propagating field is created into the waveguide, which can be decomposed along a set of spatially orthogonal modes. The amount by which a given mode is excited by the incident field $\mathbf{E}_{\mathrm{focus}}$ is determined by the scalar product of the spatial distribution for that mode and the incident field. It follows that the coupling efficiency ρ between $\mathbf{E}_{\mathrm{focus}}$ and the field $\mathbf{E}_{01}$ of the fundamental (LP_{01}) mode of the circular waveguide is given by the ratio of the integrals:

$$\rho = \frac{\left|\int_{A_\infty} \mathbf{E}_{\mathrm{focus}}\,\mathbf{E}_{01}^{*}\,\mathrm{d}A\right|^2}{\int_{A_\infty}|\mathbf{E}_{\mathrm{focus}}|^2\,\mathrm{d}A\ \int_{A_\infty}|\mathbf{E}_{01}|^2\,\mathrm{d}A}, \qquad (1)$$

where the integration domain extends at infinity in the focal plane and the symbol * denotes a complex conjugate. Since the amplitudes E_{focus} and E_{01} are each squared both in the numerator and the denominator, the ratio does

not depend on the overall field intensities and Eq. (1) is more conveniently rewritten using fields whose energies have been normalized to unity, so that

$$\rho = \left| \int_{A_\infty} \mathbf{E}_{\rm focus}\, \mathbf{E}_{01}^{*}\, \mathrm{d}A \right|^2 . \quad (2)$$

Equation (1) expresses how well the spatial distributions of the two fields match in amplitude *and* in phase. The field distribution across the LP_{01} mode is fixed and determined by the waveguide characteristics. In the case of a step-index, circular core fiber, it is given by (Gloge 1971a). In a plane transverse to the axis of the waveguide the phase is constant and the amplitude shows a symmetry of revolution, with a radial profile that extends into the cladding and can be well approximated by a Gaussian under most circumstances (Gloge 1971a, 1971b).

The field distribution at the focus of the telescope, on the other hand, is proportional to the Fourier transform of the distribution of the complex field $\mathbf{E}_{\rm pupil}$ diffracted at the entrance pupil (Born & Wolf 1980):

$$\mathbf{E}_{\rm pupil}(\boldsymbol{s}) = \mathbf{E}_\star\, \boldsymbol{\Psi}(\boldsymbol{s})\, G(\boldsymbol{s}), \quad (3)$$

where $G(\boldsymbol{s})$ is the pupil transmission function, $\mathbf{E}_\star$ the electric field amplitude received from the source at the pupil, and $\boldsymbol{\Psi}(\boldsymbol{s}) = \mathrm{e}^{j\phi(\boldsymbol{s})}$ a possible random phase mask that takes into account optical aberrations and atmospheric turbulence. The conjugated variables in the Fourier transform are the reduced coordinates $\boldsymbol{s}/\lambda$ on the pupil and the diffraction direction corresponding in the focal plane to the position $\boldsymbol{r}/f$, where f is the focal length of the telescope. A change of variables leads then to (the sign $\tilde{}$ denotes a Fourier Transform)

$$\mathbf{E}_{\rm focus}(\boldsymbol{r}) \propto \tilde{\mathbf{E}}_{\rm pupil}\left(\frac{\boldsymbol{r}}{\lambda f}\right). \quad (4)$$

2.1. Diffraction limited beams

Without turbulence nor aberrations, the phase mask at the pupil is unity: $\boldsymbol{\Psi}(\boldsymbol{s}) = 1$. The diffraction figure of an unobstructed circular aperture of radius $S_0 = d/2$ is the Airy pattern

$$\mathbf{E}_{\rm focus} \propto \mathbf{E}_\star \frac{2\,J_1(\zeta)}{\zeta}, \quad (5)$$

where ζ is the reduced radial distance to the optical axis:

$$\zeta = 2\pi\, S_0\, \frac{r}{\lambda f}. \quad (6)$$

Most often, however, a secondary mirror of radius s_0 obstructs the beam and the focal field is then expressed as ($\alpha = s_0/S_0$ is the relative obstruction of the pupil):

$$\mathbf{E}_{\rm focus} \propto \mathbf{E}_\star \left[\frac{2\,J_1(\zeta)}{\zeta} - \alpha^2\, \frac{2\,J_1(\alpha\zeta)}{\alpha\zeta}\right]. \quad (7)$$

The central obstruction can seriously damage the coupling efficiency, much more than one would expect from the loss of collecting power only. Indeed, in the focal plane

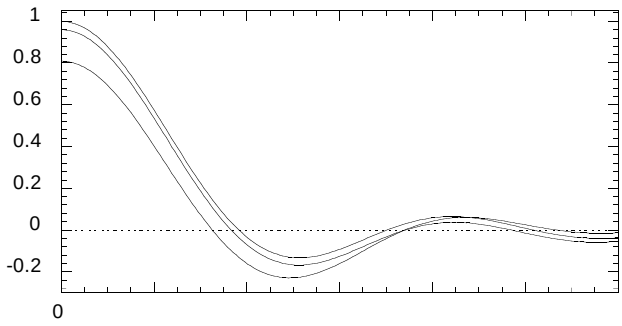

Fig. 1. Amplitude profile of the electric field at the focus of a diffraction limited telescope, for different relative central obstructions α ($\alpha = 0.436$ corresponds to the 3.60 m ESO telescope in La Silla)

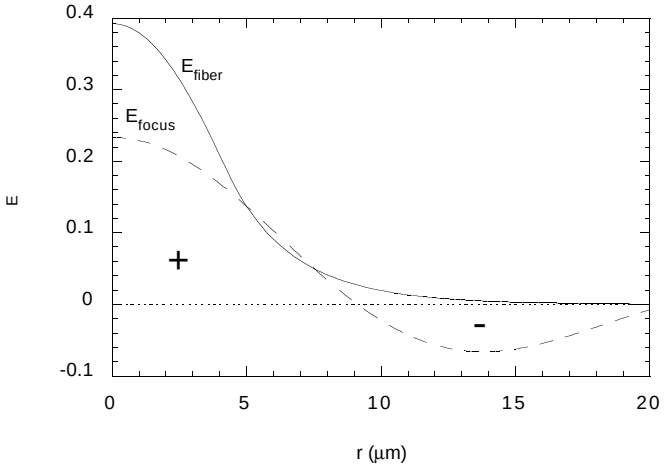

Fig. 2. Compared amplitude profiles (at wavelength $\lambda = 2.2\,\mu$m) of the electric field at the focus of a telescope ($\alpha = 0.436$, $f/d = 4$) and the fundamental mode of a fluoride glass fiber (core diameter $2a = 8.5\,\mu$m and cutoff wavelength $\lambda_{\rm c} = 1.91\,\mu$m)

the main effect of the pupil obstruction is to reinforce the first ring of the Airy pattern (Fig. 1), which contributes *negatively* to the overlap integral (Fig. 2). The coupling efficiency also depends on the input beam f-ratio. Figure 3 shows coupling efficiency vs. f-ratio curves at wavelength $\lambda = 2.2\,\mu$m for a typical fluoride glass fiber (core diameter $2a = 8.5\,\mu$m, numerical aperture $NA = 0.17$ and cutoff wavelength $\lambda_{\rm c} = 1.91\,\mu$m). For a full aperture the maximum efficiency is 78% (obtained at $f/d \simeq 3.35$), but the performance drops to 48% when the relative obstruction is $\alpha = 0.436$, as it is the case for the 3.6 m ESO telescope at La Silla observatory. Computing the curves for other fibers leads to very similar values of the maximum efficiency; however the optimum f-ratio scales like the numerical aperture of the fiber.

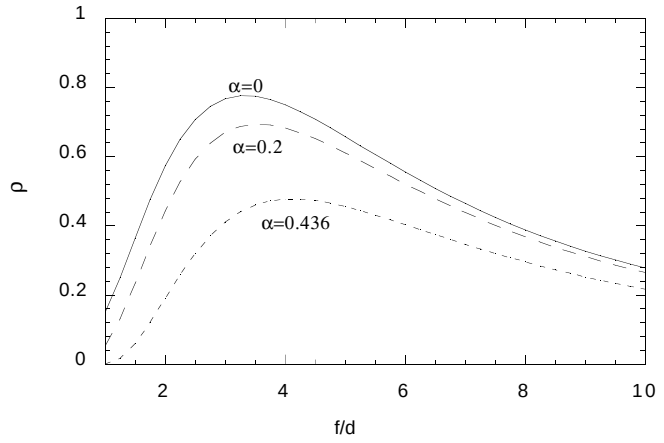

Fig. 3. Coupling efficiency into the same fluoride glass fiber as a function of the f-ratio of the input beam, for three values of the relative central obstruction α

2.2. Coupling with a turbulent wavefront

Ground-based telescopes are affected by atmospheric turbulence so that the phase of the incident wavefront is disturbed and the pupil transmission has a imaginary part. This section deals mostly with the coupling *fluctuations* in presence of turbulence. For detailed simulations of the time averaged coupling efficiency between a single-mode fiber and a turbulent wavefront, the reader is referred to (Shaklan & Roddier 1988; Ruilier 1998). Going back to Eq. (2), one can make use of Parseval's theorem to rewrite the integral in the conjugated Fourier space, i.e. the pupil plane, where we have after normalization of the field energies:

$$\rho = \left| \int_{A_\infty} \mathbf{E}_{\rm pupil}\, \tilde{\mathbf{E}}_{01}^{*}\, \mathrm{d}A \right|^2 . \tag{8}$$

Inserting the value of $\mathbf{E}_{\rm pupil}$ (Eq. 3) and developing the squared integral leads to

$$\begin{aligned} \rho \;=\; & \iint E_\star^2\, \mathbf{\Psi}(\boldsymbol{s})\, \mathbf{\Psi}^*(\boldsymbol{s'})\, G(\boldsymbol{s})\, G^*(\boldsymbol{s'}) \\ & \times \tilde{\mathbf{E}}_{01}^{*}\left(\frac{\boldsymbol{s}}{\lambda f}\right) \tilde{\mathbf{E}}_{01}\left(\frac{\boldsymbol{s'}}{\lambda f}\right) \mathrm{d}\boldsymbol{s}\, \mathrm{d}\boldsymbol{s'}. \end{aligned} \tag{9}$$

We can operate a change of variables $\boldsymbol{s}_1 = \boldsymbol{s'} - \boldsymbol{s}$ and recognize in the product $G_{\rm a}(\boldsymbol{s}) = G(\boldsymbol{s})\tilde{\mathbf{E}}_{01}(\frac{\boldsymbol{s'}}{\lambda f})$ a pupil function apodized by the Fourier transform of the fiber mode profile. Equation (9) can thus be rewritten as the integral of an autocorrelation product:

$$\begin{aligned} \rho \;&=\; E_\star^2 \int \mathrm{d}\boldsymbol{s} \int \mathbf{\Psi}(\boldsymbol{s}) \mathbf{\Psi}^*(\boldsymbol{s}_1 + \boldsymbol{s})\, G_{\rm a}(\boldsymbol{s}) G_{\rm a}^*(\boldsymbol{s_1} + \boldsymbol{s}) \mathrm{d}\boldsymbol{s}_1 \\ &=\; E_\star^2 \int A_{\mathbf{\Psi} G_{\rm a}}(\boldsymbol{s})\, \mathrm{d}\boldsymbol{s}. \end{aligned} \tag{10}$$

The autocorrelation $A_{\mathbf{\Psi}G_{\rm a}}$ of $\mathbf{\Psi}G_{\rm a}$ is nothing else than the combined MTF of the atmosphere and the apodized pupil.

2.2.1. Coupling efficiency and Strehl ratio

In adaptive optics (AO), a common criterion to assess image quality is the Strehl ratio $\mathcal{S}$ which is, for a point source, the ratio of the central intensity of the corrected image to the central intensity of an ideal, diffraction limited image of a source with the same magnitude (Born & Wolf 1980; Tyson 1991). Since the image intensity on the center is also the integral of the modulation transfer function, one has ($A_{G_{\rm a}}$ is the autocorrelation of the apodized pupil alone):

$$\begin{aligned} \mathcal{S} \;&=\; \frac{\int A_{\mathbf{\Psi}G_{\rm a}}\, \mathrm{d}\boldsymbol{s}}{\int A_{G_{\rm a}}\, \mathrm{d}\boldsymbol{s}} \\ &=\; \frac{\rho}{\rho_0}, \end{aligned} \tag{11}$$

where ρ_0 is the injection efficiency when there is no turbulence.

Thus, the injection efficiency in presence of turbulence is proportional to the Strehl ratio of the apodized pupil. In practice, if one choses a fiber with a sufficiently small core (or equivalently, if the input beam is slow enough), the coupling variations are a good estimator of the Strehl ratio fluctuations. In the image plane, one can also say that a quasi point-like fiber core samples the intensity at the center of the image, i.e. the Strehl ratio.

The combination of a single-mode fiber and a fast photometer makes up a unique tool to measure the fluctuations of the instantaneous Strehl ratio. This might be especially useful for the qualification of adaptive optics systems. An example is given in Sect. 3.

3. Experimental results

In this section, experimental data are presented which demonstrate how a single mode fiber can be used to assess the quality of a beam corrected by Adaptive Optics. We tested the coupling of a single-mode fiber to the 3.6 m ESO telescope in La Silla, equipped with the ADONIS adaptive optics system (Beuzit et al. 1997). The aim of these tests was twofold:

- To assess the gain provided by adaptive optics for the injection of starlight collected by a large pupil into a single-mode waveguide;
- To use the SM fiber, in conjunction with a fast photometer, as a "Strehl meter" to monitor the rapid fluctuations of the corrected image.

The imagery infrared channel is focused underneath the ADONIS bench where the fiber injection setup has been installed. The optical layout is shown in Fig. 4.

Description of the test bench The principle of the test is to extract part of the stellar beam to inject it into a single-mode fiber, and to perform a comparative photometry between the output of the waveguide and

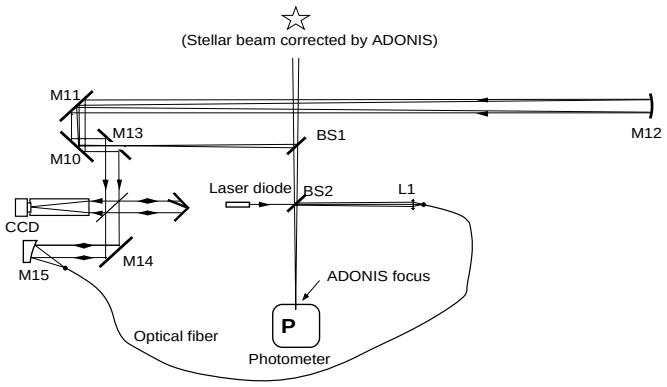

Fig. 4. Optical layout to measure the coupling efficiency of the beam corrected by ADONIS and a single-mode fiber

the direct image of the star. At the output of ADONIS, the corrected beam is thus amplitude divided on the BS1 beamsplitter:

- The transmitted beam is transmitted again through BS2 and focused directly onto the detector (an InSb photometer);
- The reflected beam goes through the holed mirror M13, is collimated by the spherical mirror M12 and injected with the off-axis parabola M15 into a small length (3 m) of single-mode infrared fiber. A control unit is also present to help register the input fiber head, whose diameter is less than 10 μm, and the star image. The output of the fiber is imaged onto the photometer by the lens L1, after a reflexion on BS2.

When the shutter located between BS1 and BS2 is closed, only the flux injected in the fiber is measured by the photometer. Conversely, the flux in the direct imagery channel can be measured by depointing the star from the fiber head. The ratio of the two fluxes provides, after calibration of the beamsplitter and additional losses (Table 1), the injection efficiency ρ.

The f-ratio of the injected beam depends on the focal lengths of the collimating mirror M12 and the off-axis parabola M15. Measurements were made at $f/d = 3$.

Injection efficiency for an internal (static) source The first coupling tests were done with an artificial source, internal to ADONIS, that presents only static aberrations. Measurements made with a circular core fiber (VF 1078, $2a = 10\,\mu$m, $ON = 0.16$) and a polarization preserving fiber (VF (MP) 1492, rectangular core $3 \times 8.5\,\mu$m) are shown in Table 2. For a 3.60 m pupil with a 1.57 m central obstruction, and a $f/d = 3$ input beam, the overlap integral (Eq. 1) of the Airy disk with the guided mode profile of the circular core fiber gives a theoretical injection efficiency $\rho_0 = 0.39$. The f-ratio of the input beam is not optimal for this fiber: the maximum efficiency $\rho_{\max} = 0.49$ is obtained for $f/d = 4.3$.

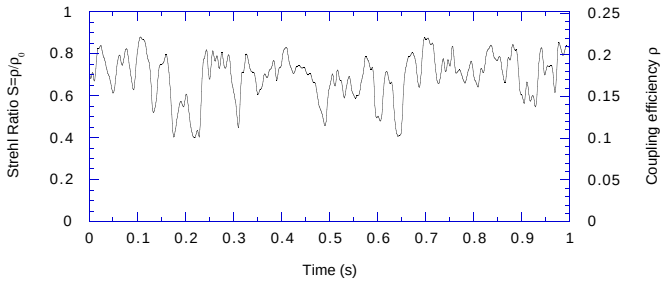

Fig. 5. Strehl ratio and injection efficiency for a stellar source (GM Lup) in a circular core fiber (VF 1078), at the 3.60 m telescope in La Silla corrected by ADONIS. Note the presence of a modulation with a 0.04 s period (25 Hz) induced by a vibration of the telescope tube. The seeing was excellent and very slow ($r_0 = 65$ cm and $\tau_0 = 0.4$ s in K). The reference efficiency for this setup was $\rho_0 = 0.25$ and was calibrated on the internal, artificial point source

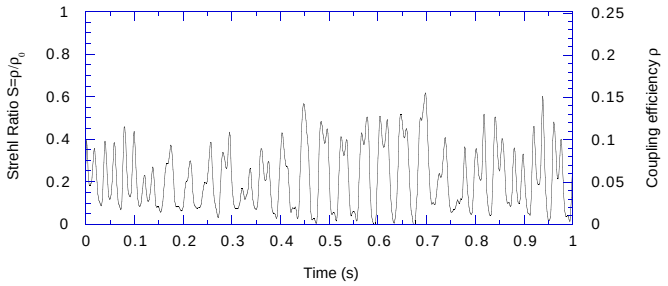

Fig. 6. Another recording of the coupling fluctuations, in identical experimental conditions. The 25 Hz modulation of the injected energy is now total

Residual aberrations in the imagery channel of ADONIS reduce the injection efficiency to below its theoretical value; by observing the image of an infrared diode set where starts the imagery channel, before observing the celestial source, one can minimize first order aberrations in this channel by introducing offsets in the interaction matrix; thus the injection efficiency depends mainly on the quality of the servo loop, which in turn depends on how well the interaction matrix between the sub-pupils slopes and the actuators was determined (Beuzit et al. 1997). The efficiency shown in the table ($\rho_0 = 0.35$) is the value obtained with the best interaction matrix obtained by ADONIS. In the worst case we found $\rho_0 = 0.20$. Finally, we found that the quality of the injection in a polarisation maintaining fiber ($\rho_0 = 0.25$) is better than what could be feared from the very elongated morphology of the core, which does not fit well an Airy disk.

Injection efficiency for a turbulent stellar source The observation of a stellar source enabled us to measure both the coupling efficiency ρ and the Strehl ratio $\mathcal{S} = \rho/\rho_0$ (Eq. 11), after calibration of ρ_0 on the static internal source ($\rho_0 = 0.25$ when ADONIS was installed at the

Table 1. Compared transmissions between the direct and the fiber channels

	Direct channel	Fiber channel
Reflexion of BS1 and BS2		$0.694 \times 0.734 = 0.509$
Transmission of BS1 and BS2	$0.306 \times 0.266 = 0.081$	
Reflexion mirrors Al		$(0.96)^6 = 0.783$
Reflexion mirrors Au		$(0.98)^2 = 0.960$
Pellicle beamsplitter transmission		0.92
Injection efficiency into the fiber		ρ
Fresnel losses at fiber/head interfaces		$(0.96)^2 = 0.922$
Signal attenuation in the fiber (30 dB/km)		0.979
Fresnel losses on lens L1		$(0.96)^2 = 0.922$
Global transmission	**0.081**	**0.293** ρ

Table 2. Coupling efficiency from a non turbulent point source with a circular core fiber (VF 1078) and a polarisation maintaining fiber (VF (MP) 1492)

Fiber		ρ_0
VF 1078	Theoretical efficiency	0.39
VF 1078	Measured efficiency (with static correction of the aberrations)	0.35
VF 1078	Measured efficiency (without aberration correction)	0.29
VF (MP) 1492	Measured efficiency (with static correction of the aberrations)	0.25

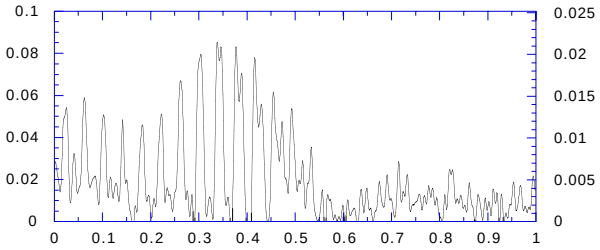

Fig. 7. Strehl ratio and injection efficiency for a stellar source (GM Lup) in a circular core fiber (VF 1078), at the uncorrected 3.60 m telescope in La Silla

telescope). Thus for the first time it was possible to follow the fast fluctuations of the Strehl ratio in an image corrected by adaptive optics (Figs. 5 and 6). The coupled flux was found to be modulated with a period of 0.04 s, whose instrumental origin was clearly testified. The intensity of the 25 Hz component depended on the pointing direction of the telescope, but the vibration was still present when the AO was turned off (Fig. 7). It was concluded that the whole telescope tube vibrated at a rate too fast to be compensated by the tip-tilt mirror of the AO system. The fact that the modulation can reach 100% (as is the case in Fig. 6) means that the vibration amplitude can be greater than the diameter of an Airy disk in K, i.e. 150 mas. When ADONIS is used for long exposure imaging as it is the case usually, the vibration cannot be directly detected, but induces a degradation of the Strehl ratio that can reach 70%. The frequency of 25 Hz (or 24.8 Hz as was later measured) was connected to a natural resonance frequency of the telescope mount, and following this diagnosis the problem was fixed.

Still, despite this limitation, the use of AO led to a major improvement of the time averaged Strehl ratio: $\langle \mathcal{S} \rangle = 0.22$ (Fig. 5) to 0.70 (Fig. 6), depending on the modulation intensity, compared to an average Strehl ($\langle \mathcal{S} \rangle = 0.019$) without AO. The gain in coupling efficiency provided by the correction can therefore reach a factor $0.70/0.019 = 37$. In the best cases, more than 20% of the stellar light collected by the 3.6 m telescope mirror was injected into the single-mode fiber, which is more than half the theoretical maximum expected of 39% for that telescope. Extrapolating this experimental result to a vibration-free VLT where the 8 m pupils feature

a proportionally small (1.2 m) central obstruction (hence an expected theoretical maximum of 76%), one can predict that actual injection efficiencies of 40% should be achievable with very large telescopes.

4. Conclusion

The price to pay for the perfect spatial filtering of a single-mode fiber is a loss of photons. To obtain the best possible coupling efficiency (78%) one needs a diffraction-limited beam with no central obstruction; yet, even in perfect imaging conditions, the central obstruction of the secondary in most 4-meter class telescopes reduces the maximum efficiency down to 42%. When the central obstruction ratio is less than 20%, which is the case for the new generation of 8 m class telescopes, this reduction remains acceptable.

When the fiber is fed with turbulent starlight, then the coupled power displays strong temporal fluctuations. It was shown that the coupling efficiency is then directly linked to the Strehl ratio of the image, or equivalently, to the integral of the pupil autocorrelation. The total amount of energy that can be injected into the fiber is thus limited by the size r_0 of a coherence area on the pupil.

For a large telescope ($d \gg r_0$) the coupling efficiency can be dramatically improved by (at least partially) correcting the incoming wavefront with adaptive optics. Measuring this efficiency is also an excellent means to monitor the real-time performance of an adaptive optics system. This is how the coupling of a single-mode fiber to the ADONIS adaptive optics system on the 3.6 m ESO telescope in La Silla enabled us to detect an instrumental periodic perturbation at 25 Hz, which was too fast to have been detected otherwise, yet which was strong enough to induce up to a 70% degradation of the average Strehl ratio. Thus it appears that single-mode fibers can be a unique tool to assess the dynamic evolution of the optical quality in modern telescopes.

References

Beuzit J.-L., Demailly L., Gendron E., et al., 1997, Adaptive Optics on a 3.6-Meter Telescope, The ADONIS System, Ex. A. 7, p. 285–292

Born M., Wolf E., 1980, Principle of Optics. Pergamon Press, Oxford

Coudé du Foresto V., Ridgway S., Mariotti J.M., 1997, A&AS 121, 379

Ge J., Angel J.R.P., Shelton C., 1998, Proc. SPIE 3355, 253

Gloge D., 1971, Appl. Opt. 10, 2442

Gloge D., 1971, Appl. Opt. 10, 2252

Jeunhomme L., Single mode fiber optics, Principles and applications. Marcel Dekker, New-york

Neumann E.G., Single mode fibers. Springer-Verlag, Berlin

Roddier F., 1987, J. Opt. Soc. Am. A 4, 1396

Ruilier C., 1998, in "Astronomical Interferometry", Proc. SPIE 3350, Reasenberg R.D. (ed.), p. 319

Shaklan S.B., 1989, Ph.D. Thesis, Univ. of Arizona

Shaklan S.B., Roddier, 1988, App. Opt. 27, 2334

Tyson S., 1991, "Principles of adaptive optics". Academic Press, inc.